Systems Chemistry

Deutsche Ausgabe: DOI: 10.1002/ange.201503898
Internationale Ausgabe: DOI: 10.1002/anie.201503898

A Bistable Switch in Dynamic Thiodepsipeptide Folding and Template-Directed Ligation

*Rakesh Mukherjee, Rivka Cohen-Luria, Nathaniel Wagner, and Gonen Ashkenasy**

Abstract: *Bistable reaction networks provide living cells with chemically controlled mechanisms for long-term memory storage. Such networks are also often switchable and can be flipped from one state to the other. We target here a major challenge in systems chemistry research, namely developing synthetic, non-enzymatic, networks that mimic such a complex function. Therefore, we describe a dynamic network that depending on initial thiodepsipeptide concentrations leads to one of two distinct steady states. This bistable system is readily switched by applying the appropriate stimuli. The relationship between the reaction network topology and its capacity to invoke bistability is then analyzed by control experiments and theory. We suggest that demonstrating bistable behavior using synthetic networks further highlights their possible role in early evolution, and may shine light on potential utility for novel applications, such as chemical memories.*

Key milestones in systems chemistry have been realized in recent years by the de novo design and analysis of synthetic chemical networks manifesting increasingly complex functions. Networks of different characteristics have been used to afford such functions, including dynamic libraries under thermodynamic control,[1] replication networks under kinetic control,[2] and as recently demonstrated, dynamic mixtures incorporating catalytic[3] and autocatalytic[4] processes, leading to reactions progress under "partial thermodynamic control".[5] Among other features, such networks display various motifs, such as hubs, and sub-network modularity.[2a] They are furthermore adaptive in response to chemical and physical triggers,[4d,e,6] and facilitate the emergence of functional kinetically trapped architectures.[7] A major, generally unmet, challenge is to develop the synthetic, non-enzymatic, networks to mimic significantly more complex functionality observed in cell biology, such as displaying oscillation and bistability (or multistability).[8] Achieving this task will highlight possible roles for molecular networks in early evolution and at the same time can shine light on their utility for novel applications in material science.

Cellular reaction networks often display bistability. Such a phenomenon simply means that a dynamic system has two stable resting states. These states are not necessarily symmetric with respect to the stored energy. Bistability provides the cell with a mechanism for long-term memory storage, namely the ability to integrate a transient molecular stimulus into a sustained molecular response.[9] Hence, these biological systems are also switchable; they can be flipped from one state to the other by application of specific stimuli. Using synthetic biology, several networks were constructed to create a toggle switch by rearranging regulatory components in cells.[10] A bottom-up design approach—more relevant for the current research—was also applied to produce bistable molecular arrays as memory devices and switches. Recent examples used different chemical systems, such as the Belousov–Zhabotinsky reaction-diffusion systems,[11] enzyme feedback-driven assemblies in solution and gels,[12] and DNA (and enzymes) in vitro circuits.[9a,13] As part of a long-term program to study the complexification of synthetic peptide-based networks and its possible relevance for early evolution, we describe here a dynamic reaction network that, depending on initial thiodepsipeptide concentrations, leads to one of two distinct steady-state (SS) concentration distributions. The newly developed bistable system can be switched from one state to the other by applying physical (heat) or chemical stimuli; it presents an unprecedented bistable switch operating with non-enzymatic catalysis. Since a great deal of subtlety exists in the relationship between the structure of a reaction network and its capacity to invoke bistability,[9b,14] we characterize the network functionality under various different conditions. First, we follow the bistability and switch operation under a range of working concentrations. Then, using additional control experiments and an extensive theoretical analysis, we highlight the most prevalent mechanistic features that affect bistability and its scope.

The bistable system was studied by following the reversible formation of a thioester peptide **R** from its precursor peptides, a shorter thioester, **E**, and a thiol-terminated, **N** (Figure 1). Peptide **R** forms a trimeric coiled-coil structure in neutral pH aqueous solutions (see Figure S1 in the Supporting Information),[15] and can serve as a template for the association of **E** and **N**, enhancing their ligation by a thiol-thioester exchange reaction.[4e,g] As was shown for other thioester peptides,[16] we have recently elucidated that the formation of a well-folded coiled-coil structure by **R** renders it stable against the attack of peptide or small-molecule thiols, thus significantly slowing down its decomposition, relative to the decomposition of unfolded peptides or peptides that form less stable coiled coils.[15] This observation implies a disparity in rates of formation/decomposition of **R** in the autocatalyzed and uncatalyzed reactions. Based on earlier theoretical predictions that even traditional (mass-action) kinetics, with a disparity in conversion of just one or two substrates, already carries the capacity for bistability,[14] and that hysteresis is

[*] R. Mukherjee, Dr. R. Cohen-Luria, Dr. N. Wagner, Prof. G. Ashkenasy
Department of Chemistry, Ben Gurion University of the Negev
Be'er Sheva, 84105 (Israel)
E-mail: gonenash@bgu.ac.il

Supporting information for this article is available on the WWW under http://dx.doi.org/10.1002/anie.201503898.

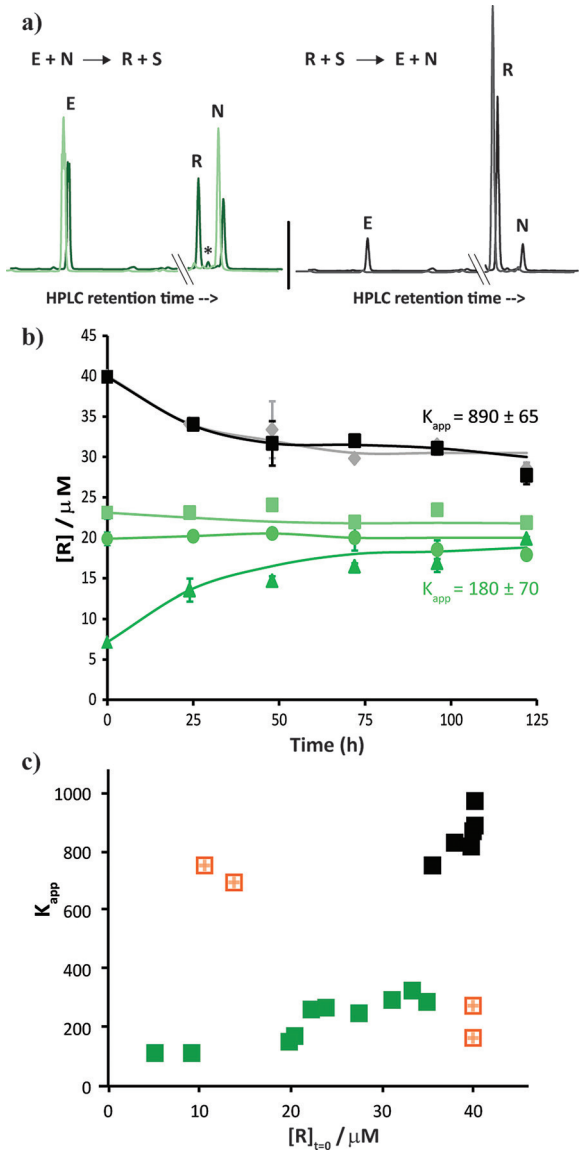

Figure 1. Time-dependent and steady-state analysis of reactions between **E**, **N**, **R**, and **S**, initiated with different concentration combinations. In all cases [**E**] = [**N**], [**E** + **R**] = 40 μM, and **S** in large excess (ca. 3 mM; Table S1). a) HPLC traces for two representative experiments initiated with mixtures containing **E** and **N** (left), or **R** (right). Light color used for chromatograms obtained at initial states (t = 15 s) and dark color chromatograms for SS ($t \geq 72$ h). The slight offset between chromatograms is provided for better clarity. *marks a residual N disulfide peak. b) **R** concentrations as a function of time for representative reactions leading to low (green traces) or high (black/gray) SS concentration distributions. The K_{app} values ([**R**][**S**]/[**E**][**N**]) are given for average measured concentrations of the presented data. c) K_{app} values as function of the initial concentration of **R**, highlighting low (green) and high (black) SS distributions. The square orange color marks are shown for the low-to-high ($[\mathbf{R}]_{t=0}$ = 10.5 and 14 μM) and high-to-low ($[\mathbf{R}]_{t=0}$ = 40 μM) switching experiments (see text). Peptide sequences: **E** = Ar-RVARLEKKVSALEKKVA-COSR, **N** = H-ZLEXEVARLKKLVGE-$CONH_2$, **R** = Ar-RVARLEKKVSALEKKVAZLEXEVA-RLKKLVGE-$CONH_2$. Ar = 4-acetamidobenzoate, Z = -SCH_2CO, X = Lys-Ar, SR = 2-mercaptoethane sulfonate. Reactions were carried out in 3-(*N*-morpholino)propanesulfonic acid (MOPS) buffer pH 7.0 ± 0.1, at room temperature (22 ± 1 °C), and with tris(2-carboxyethyl)phosphine (TCEP) as reducing agent and 4-acetamido-benzoic acid as an HPLC internal standard.

a marker for complex landscapes in protein folding,[17] we hypothesize that the reversible formation of **R** from **E** and **N** may follow different pathways leading to bistability. Figure 1 shows the equilibration kinetics (Figure 1b) and the steady-state (SS) product distributions observed for multiple reactions having the same total material concentrations ([**E**] + [**R**] = 40 μM; Figure 1c). It is clearly observed that reactions initiated with substrates only, or in the presence of low **R** concentrations, reached a low SS (apparent equilibrium distribution $K_{app} = [\mathbf{R}][\mathbf{S}]/[\mathbf{E}][\mathbf{N}] \approx 200$), while reactions initiated with only **R**, or in the presence of low **E** and **N** concentrations, reached a much higher SS ($K_{app} > 800$). Figure 1c allows us to closely pinpoint the SS transition value at $34 < [\mathbf{R}]_{t=0} < 35.5$ μM.

The equilibration experiments were then repeated with reaction mixtures containing different total concentrations, ranging at 25–150 μM (Figure 2). In all cases, a clear bistability picture was obtained, revealing SS equilibration with two significantly distinct K_{app} values, each of narrow distribution (see standard-deviation bars in Figure 2). Interestingly, when the system was studied with increased total concentrations, the results show a small increase in the low K_{app} values and a larger increase in the high K_{app}.

An additional set of experiments was conducted to highlight the role that **R** coiled-coil formation plays in the observed equilibration pattern. First, circular dichroism (CD) measurements (Figure S1 and Table S2) revealed that **R** can assemble into highly helical (> 67 %) coiled-coil structures at almost the entire range of studied concentrations (10–150 μM), and that **E** and **N** present as random coils even at high concentrations (100 μM). This data supports our hypothesis that the bistable behavior is a result of an emerged

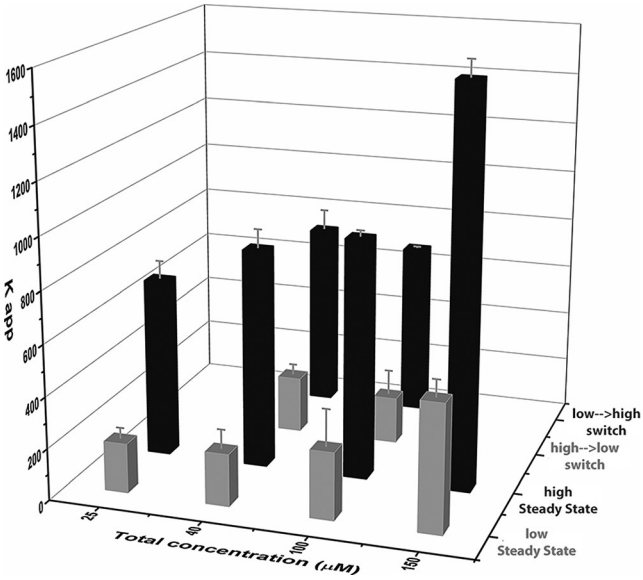

Figure 2. K_{app} values as a function of the total (**E** + **R**) concentrations, highlighting low (gray) and high (black) steady-state distributions. Results from the high-to-low and low-to-high switching experiments are shown for total concentrations of 40 μM and 100 μM. Reaction conditions were as described in Figure 1. Table S1 lists all initial and SS concentrations, calculated at $t \geq 72$ h.

phenomenon related to the topology of the small network of interactions at each studied concentrations combination. In a second experiment, we reacted **E** and **N**, or **R**, in the presence of high concentration of the denaturing reagent GnHCl, and in the third, we reacted short peptides that do not fold to defined structures (**Es** and **Ns**, or **Rs**; see the Supporting Information). Significantly, in both cases, the reaction mixtures equilibrated into a single SS with low product (**R** or **Rs**) concentrations (Figure S2 and Table S1).

The system equilibration into two distinct steady states reflects the bistable behavior, obtained because of decoupling of the trimeric **R** unfolding events from its **S**-dependent decomposition reaction leading to **E** and **N**. We have studied the possibility of switching the system between the two states by external energy supply (Scheme 1). After noting that

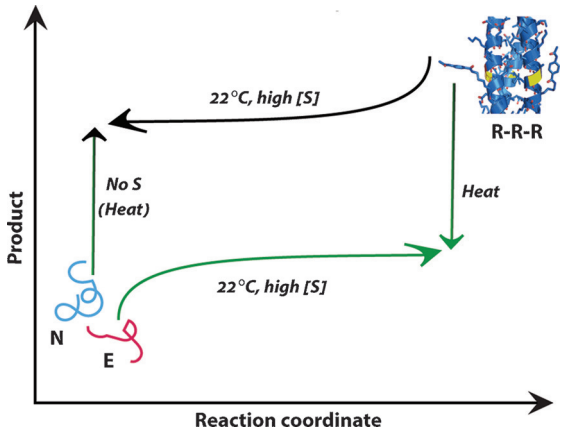

Scheme 1. Bistable behavior observed along **R** thiodepsipeptide equilibration experiments described in Figures 1 and 2. The system can be switched between the two SSs by applying heat, or by initiating the forward reaction in the absence of **S** molecules.

equilibration at higher temperature (37 °C) leads to lower SS product distributions (all $K_{app} < 100$; Figure S2), and apparently a less clear-cut bistability picture, we devised a high-to-low SSs temperature-dependent switch. The reaction mixtures ($[\mathbf{R}+\mathbf{E}] = 40$ or 100 μM) containing high initial **R** concentrations were allowed to react for 40 h at 37 °C, and then re-equilibrated at room temperature, reaching the low steady state (Figures 1c and 2). The low-to-high SS switch was chemically achieved, by first allowing mixtures containing **E** and **N** to react in the absence of the thiol small-molecule—reflecting a chemical switch for the forward reaction—affording formation of high **R** concentrations within 1 day. These mixtures were then equilibrated in the presence of excess thiol and found stable against degradation, reaching the high SS (Figures 1c and 2).

In order to further probe the interplay between multiple network reactions affecting the rate of **R** thioester formation and the system bistability capacity, we model the overall process [Eqs. (1)–(3)]. These equations account for the template-free reaction between E and N [Eq. (1)], their template-assisted ligation enhanced by a dimer TT [Eq. (2)], and the reversible template association into dimer and trimer species [Eq. (3)]. The concentration of R, which is measured experimentally, is derived from the template (T) concentrations in all of its forms [Eq. (4)].

$$E + N \underset{\langle g \rangle}{\overset{g}{\rightleftharpoons}} T + S \tag{1}$$

$$E + N + TT \underset{\langle a \rangle}{\overset{a}{\rightleftharpoons}} [ENTT] \underset{\langle b \rangle}{\overset{b}{\rightleftharpoons}} TTT + S \tag{2}$$

$$TTT \underset{\langle f \rangle}{\overset{f}{\rightleftharpoons}} T + TT \underset{\langle d \rangle}{\overset{d}{\rightleftharpoons}} T + T + T \tag{3}$$

$$[R] = [T] + 2[ENTT] + 2[TT] + 3[TTT] \tag{4}$$

In order to predict the SS positions, we compute the rate of each process using mass-action kinetics. Assuming fast intermediate equilibrium, in which the assembly processes reach SS faster than the ligation processes,[1c,18] and practical $\langle b \rangle = 0$, it can be shown that the intermediate concentrations are continually related in the following manner: $[TT] \approx [T]^2$ and $[ENTT] \approx [E][N][T]^2$. This yields the approximate rate equation for R production as in Equation (5) ($c = a\,b\,\langle d \rangle / (\langle a \rangle + b)\,d$); SS is reached when this rate equals zero (Figure S3).

$$\frac{d[R]}{dt} \approx g[E][N] - \langle g \rangle [T][S] + c[E][N][T]^2 \tag{5}$$

Equation (5) reflects that the rate is not a monotonic function of $[R]$, and accordingly, there may be several SSs for given initial conditions. Furthermore, each SS point may be stable or unstable, based on the Jacobian ($d^2[R]/dt^2$).[19] Figure 3 shows the computed SS solutions for (normalized) R for various sets of rate constants. It can be seen that for certain total resource regimes there may be three solutions: two represent stable points—gray and black for low and high solutions, respectively—while the third in between the other two, is unstable (dashed). In the latter cases, initial R concentrations less than the unstable point converge to the lower stable point, while initial R concentrations greater than the unstable point converge to the higher stable point.

Figure 3a shows the results for standard initial concentrations and rate constants, corresponding to nominal experimental conditions.[20] The experimentally observed bistable behavior is qualitatively reproduced here for total concentrations between approximately 45 μM and 140 μM. For total concentrations less than 45 μM or greater than 140 μM, the system has only one SS solution, revealing that these values are the bifurcation points. Interestingly, the bifurcation points can also be predicted mathematically as a function of the rate constants and S concentrations (see the Supporting Information); for the case shown in Figure 3a, such prediction yielded 39 μM and 146 μM, respectively. The theoretical model allows us to test the effect of additional parameters on the bistability behavior. Figure 3b displays the numerical results for rate constants corresponding to the control experiments under unfolding conditions, which yielded a single low SS point (Figure S2). Higher values were applied for the dissociation constants ($\langle a \rangle$, d and f) relevant for this case. The bifurcation map demonstrates that the bistability regime has shifted to much higher values of total resources (700–1200 μM). Using

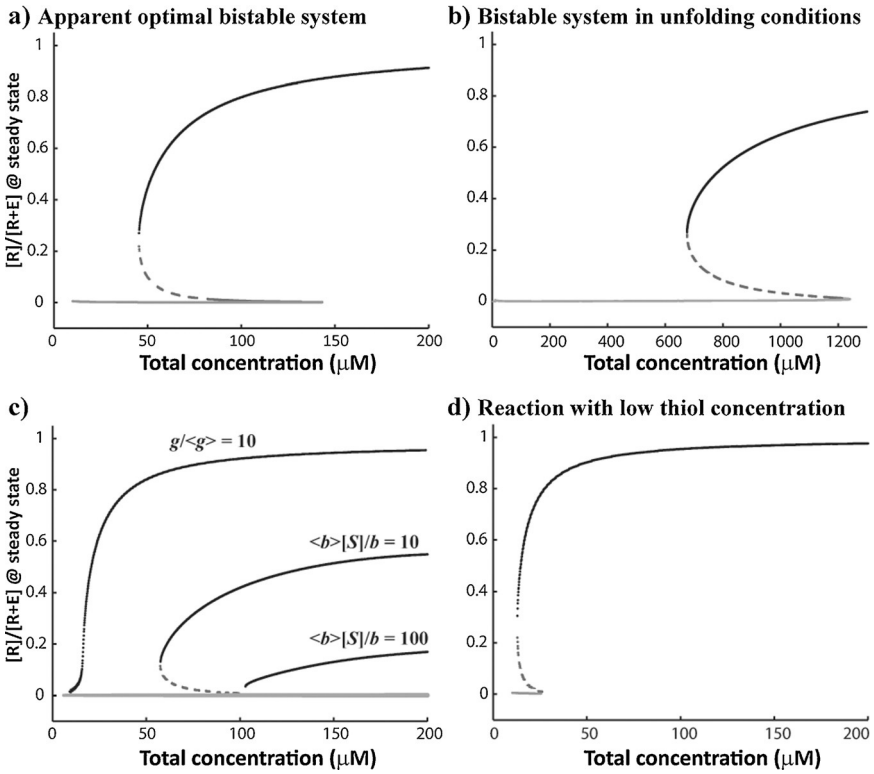

Figure 3. Normalized SS solutions for R as a function of total $R+E$ concentration, computed numerically by zeroing the rate of product formation [Eqs. (5) or (6)]. The stable SS are displayed in gray (low solution) and black (high solution), while the unstable solutions are shown by dashed lines. In all cases, $[E]=[N]$. a) Reactions under standard initial concentrations and rate constants, corresponding to nominal experimental conditions: $a=10^9$, $\langle d\rangle=\langle f\rangle=10^6$, $\langle a\rangle=10$, $d=10$, $f=1000$, $g=1$, $b=10$, $\langle g\rangle=100$, $[S]=3000$ μM. b) Results for reactions with rate constants corresponding to the control experiments in unfolding conditions: $\langle a\rangle=1000$, $d=1000$, $f=100\,000$. c) A set of reactions reflecting irreversible R formation ($g/\langle g\rangle=10$) and three cases of fully-reversible template-assisted reaction step ($\langle b\rangle[S]/b=10$, 100 or 1000). All these cases lead to diminished or no bistability. d) Reactions with the standard parameters, but with $[S]=100$ μM.

the data shown in Figure 3c, we then analyze the delicate balance between various reversible processes needed to obtain bistable behavior. First, we reveal that a (practically) irreversible system, in which the background forward ligation is much preferred over the back reaction ($g/\langle g\rangle=10$), leads to a single SS. Additionally, the results for three distinct values of $\langle b\rangle$, reflecting systems driven by a fully reversible template-assisted reaction step, show that bistability is also diminished. The rate equation for this system is given by Equation (6) (see the Supporting Information).

$$\frac{d[R]}{dt}\approx g[E]\,[N]-\langle g\rangle[T]\,[S]+b\,[ENTT]-\langle b\rangle\,[TTT]\,[S] \qquad (6)$$

The lower solution is common to all three values, while the higher solutions decrease with increasing $\langle b\rangle$, highlighting that indeed the experimental system is better represented by our original model where only the background reaction is reversible. Finally, Figure 3d highlights the need for high excess of S molecule to afford the bistable behavior. Here, when the same nominal rate constants were applied with drastically reduced concentration of S (100 μM), the bistability was almost completely reduced, namely that the higher solution dominated as in the low-to-high switch experiment (Figures 1c and 2).

The bistable system emerged because of disparity in the different reaction rates associated with competing folding and assembly–disassembly processes. Several recent reports have suggested that de novo designed chemical systems operating out-of-equilibrium can give rise to additional emergent behavior including oscillations.[8,20b,21] We now suggest that bistability may also exist in dynamic libraries incorporating catalytic reactions. If proven viable, such systems might be used to develop and analyze dynamic memory devices.

Acknowledgements

This research was supported by the European Research Council (ERC grant number 259204). We acknowledge ITN ReAd support (R.M.), and the COST action CM1304. We thank Prof. Enrique Peacock-Lopez (Williams College) and Sagi Kraun for scientific discussions, and Dr. Zehavit Dadon for help in the early stages.

Keywords: bistability · depsipeptides · reaction networks · systems chemistry

How to cite: *Angew. Chem. Int. Ed.* **2015**, *54*, 12452–12456
Angew. Chem. **2015**, *127*, 12629–12633

[1] a) J. Li, P. Nowak, S. Otto, *J. Am. Chem. Soc.* **2013**, *135*, 9222–9239; b) J.-M. Lehn, *Angew. Chem. Int. Ed.* **2013**, *52*, 2836–2850; *Angew. Chem.* **2013**, *125*, 2906–2921; c) K. Severin, *Chem. Eur. J.* **2004**, *10*, 2565–2580; d) L. J. Prins, *Chim. Ind.* **2010**, *92*, 126–131.

[2] a) Z. Dadon, N. Wagner, G. Ashkenasy, *Angew. Chem. Int. Ed.* **2008**, *47*, 6128–6136; *Angew. Chem.* **2008**, *120*, 6221–6230; b) A. Vidonne, D. Philp, *Eur. J. Org. Chem.* **2009**, 583–588; c) O. Taran, G. von Kiedrowski, *Chem. Synth. Biol.* **2011**, 289–319; d) A. J. Bissette, S. P. Fletcher, *Angew. Chem. Int. Ed.* **2013**, *52*, 12800–12826; *Angew. Chem.* **2013**, *125*, 13034–13061.

[3] a) R. J. Williams, A. M. Smith, R. Collins, N. Hodson, A. K. Das, R. V. Ulijn, *Nat. Nanotechnol.* **2009**, *4*, 19–24; b) V. T. Bhat, A. M. Caniard, T. Luksch, R. Brenk, D. J. Campopiano, M. F. Greaney, *Nat. Chem.* **2010**, *2*, 490–497; c) B. Rasmussen, A. Sorensen, H. Gotfredsen, M. Pittelkow, *Chem. Commun.* **2014**, *50*, 3716–3718.

[4] a) J. W. Sadownik, D. Philp, *Angew. Chem. Int. Ed.* **2008**, *47*, 9965–9970; *Angew. Chem.* **2008**, *120*, 10113–10118; b) S. Xu, N.

Giuseppone, *J. Am. Chem. Soc.* **2008**, *130*, 1826 – 1827; c) V. del Amo, D. Philp, *Chem. Eur. J.* **2010**, *16*, 13304 – 13318; d) J. M. A. Carnall, C. A. Waudby, A. M. Belenguer, M. C. A. Stuart, J. J. P. Peyralans, S. Otto, *Science* **2010**, *327*, 1502 – 1506; e) Z. Dadon, M. Samiappan, N. Wagner, G. Ashkenasy, *Chem. Commun.* **2012**, *48*, 1419 – 1421; f) M. Malakoutikhah, J. J. P. Peyralans, M. Colomb-Delsuc, H. Fanlo-Virgos, M. C. A. Stuart, S. Otto, *J. Am. Chem. Soc.* **2013**, *135*, 18406 – 18417; g) Z. Dadon, N. Wagner, S. Alasibi, M. Samiappan, R. Mukherjee, G. Ashkenasy, *Chem. Eur. J.* **2015**, *21*, 648 – 654.

[5] A. Eschenmoser, *Science* **1999**, *284*, 2118 – 2124.

[6] a) J. Atcher, A. Moure, J. Bujons, I. Alfonso, *Chem. Eur. J.* **2015**, *21*, 6869 – 6878; b) M. Samiappan, Z. Dadon, G. Ashkenasy, *Chem. Commun.* **2011**, *47*, 710 – 712; c) G. Leonetti, S. Otto, *J. Am. Chem. Soc.* **2015**, *137*, 2067 – 2072.

[7] a) E. Mattia, S. Otto, *Nat. Nanotechnol.* **2015**, *10*, 111 – 119; b) B. Rubinov, N. Wagner, M. Matmor, O. Regev, N. Ashkenasy, G. Ashkenasy, *ACS nano* **2012**, *6*, 7893 – 7901; c) P. A. Korevaar, T. F. A. de Greef, E. W. Meijer, *Chem. Mater.* **2014**, *26*, 576 – 586.

[8] I. R. Epstein, *Chem. Commun.* **2014**, *50*, 10758 – 10767.

[9] a) A. Padirac, T. Fujii, Y. Rondelez, *Proc. Natl. Acad. Sci. USA* **2012**, *109*, 19047 – 19048; b) T. Wilhelm, *BMC Syst. Biol.* **2009**, *3*, 90.

[10] a) T. S. Gardner, C. R. Cantor, J. J. Collins, *Nature* **2000**, *403*, 339 – 342; b) M. R. Atkinson, M. A. Savageau, J. T. Myers, A. J. Ninfa, *Cell* **2003**, *113*, 597 – 607.

[11] a) R. J. Olsen, I. R. Epstein, *J. Chem. Phys.* **1991**, *94*, 3083 – 3095; b) A. Kaminaga, V. K. Vanag, I. R. Epstein, *Angew. Chem. Int. Ed.* **2006**, *45*, 3087 – 3089; *Angew. Chem.* **2006**, *118*, 3159 – 3161.

[12] a) G. Hu, J. A. Pojman, S. K. Scott, M. M. Wrobel, A. F. Taylor, *J. Phys. Chem. B* **2010**, *114*, 14059 – 14063; b) F. Muzika, T. Bansagi, I. Schreiber, L. Schreiberova, A. F. Taylor, *Chem. Commun.* **2014**, *50*, 11107 – 11109.

[13] a) J. Kim, S. White Kristin, E. Winfree, *Mol. Syst. Biol.* **2006**, *2*, 68; b) T. Lebar, U. Bezeljak, A. Golob, M. Jerala, L. Kadunc, B. Pirs, M. Strazar, D. Vucko, U. Zupancic, M. Bencina, V. Forstneric, R. Gaber, J. Lonzaric, A. Majerle, A. Oblak, A. Smole, R. Jerala, *Nat. Commun.* **2014**, *5*, 5007.

[14] G. Craciun, Y. Tang, M. Feinberg, *Proc. Natl. Acad. Sci. USA* **2006**, *103*, 8697 – 8702.

[15] Z. Dadon, M. Samiappan, A. Shahar, R. Zarivach, G. Ashkenasy, *Angew. Chem. Int. Ed.* **2013**, *52*, 9944 – 9947; *Angew. Chem.* **2013**, *125*, 10128 – 10131.

[16] M. G. Woll, S. H. Gellman, *J. Am. Chem. Soc.* **2004**, *126*, 11172 – 11174.

[17] a) B. T. Andrews, D. T. Capraro, J. I. Sulkowska, J. N. Onuchic, P. A. Jennings, *J. Phys. Chem. Lett.* **2013**, *4*, 180 – 188; b) M. Shigeno, Y. Kushida, M. Yamaguchi, *Chem. Commun.* **2015**, *51*, 4040 – 4043.

[18] G. von Kiedrowski, *Bioorg. Chem. Front.* **1993**, *3*, 113 – 146.

[19] a) K. M. Beutel, E. Peacock-Lopez, *J. Chem. Phys.* **2006**, *125*, 024908; b) *An Introduction to Nonlinear Chemical Dynamics: Oscillations, Waves, Patterns, and Chaos* (Eds.: I. R. Epstein, J. A. Pojman), Oxford University Press, New York, **1998**.

[20] a) N. Wagner, G. Ashkenasy, *Chem. Eur. J.* **2009**, *15*, 1765 – 1775; b) N. Wagner, S. Alasibi, E. Peacock-Lopez, G. Ashkenasy, *J. Phys. Chem. Lett.* **2015**, *6*, 60 – 65.

[21] a) S. Soh, M. Byrska, K. Kandere-Grzybowska, B. A. Grzybowski, *Angew. Chem. Int. Ed.* **2010**, *49*, 4170 – 4198; *Angew. Chem.* **2010**, *122*, 4264 – 4294; b) T. Le Saux, R. Plasson, L. Jullien, *Chem. Commun.* **2014**, *50*, 6189 – 6195; c) L. Gurevich, R. Cohen-Luria, N. Wagner, G. Ashkenasy, *Chem. Commun.* **2015**, *51*, 5672 – 5675.

Received: April 23, 2015
Revised: July 21, 2015
Published online: September 4, 2015

